Contents lists available at ScienceDirect

Biotechnology Reports

Research Article

Cu₂O nanoparticles synthesized by green and chemical routes, and evaluation of their antibacterial and antifungal effect on functionalized textiles

David Asmat-Campos [a,d,*], Gabriela Montes de Oca-Vásquez [b], Jesús Rojas-Jaimes [a,c], Daniel Delfín-Narciso [d], Luisa Juárez-Cortijo [d], Renny Nazario-Naveda [d,e], Diego Batista Menezes [b], Reinaldo Pereira [b], Marcos Simbrón de la Cruz [f]

[a] *Universidad Privada del Norte, Dirección de Investigación, Innovación & Responsabilidad Social, Trujillo, Perú*
[b] *Laboratorio Nacional de Nanotecnología, Centro Nacional de Alta Tecnología, 10109 Pavas, San José, Costa Rica*
[c] *Facultad de Ciencias de la Salud, Universidad Privada del Norte, Av. El Sol 461, San Juan de Lurigancho, Lima, 15434, Perú*
[d] *Grupo de Investigación en Ciencias Aplicadas y Nuevas Tecnologías, Universidad Privada del Norte, Trujillo, Perú*
[e] *Universidad Autónoma del Perú, Lima, Perú*
[f] *Universidad Privada Norbert Wiener, Lima, Perú*

ARTICLE INFO

ABSTRACT

The potential for the application of metal-containing nanomaterials at the nanoscale promotes the opportunity to search for new methods for their elaboration, with special attention to those sustainable methods. In response to these challenges, we have investigated a new method for green synthesis of cuprous oxide nanoparticles (Cu₂O NPs) using *Myrciaria dubia* juice as an organic reductant and, comparing it with chemical synthesis, evaluating in both cases the influence of the volume of the organic (juice) and chemical (ascorbic acid) reductants, for which a large number of techniques such as spectrophotometry, EDX spectrometry, TEM, SEM, DLS, FTIR spectroscopy have been used. Likewise, the nanomaterial with better morphological characteristics, stability, and size homogeneity has been applied in the functionalization of textiles by means of in situ and post-synthesis impregnation methods. The success of the synthesis process has been demonstrated by the antimicrobial activity (bacteria and fungi) of textiles impregnated with Cu₂O NPs.

1. Introduction

Nanomaterials, considered as such because of the range of their dimensions between 1 and 100 nm, are the object of study of current research due to the new characteristics of these materials and their potential applications in areas such as medicine [1,2], industry [3,4], agriculture [5], biosensors, among others [6–8]. However, technological progress has also led to a change in the characteristics of particle contamination, especially those of nanometric sizes, as they generate new and varied chemical compositions, requiring an intelligent design that not only offers benefits but also limits adverse impacts on health and the ecosystem [9–11].

In recent years, research has been focused on the production of nanoparticles (NPs) using eco-friendly methods, where synthetic chemicals are being replaced by organic compounds in charge of the precursor reduction process, the latter being economical and producing fewer polluting residues. "Green" methods using extracts of leaves, fruits, stems, and bark of various plants are among the most commonly used [12–14]. The polyphenolic compounds, reducing sugars and amino acids present in these extracts, are indicated as those responsible for the process of reduction and formation of nanoparticles [15,16].

Copper is a very accessible material because it is inexpensive and abundant compared to noble metals such as gold or silver, and together with its antimicrobial and antifungal properties, it is an excellent candidate for several industrial and medical applications. Studies on cuprous oxide nanoparticles (Cu₂O NPs) synthesized from copper salt and Ascorbic Acid (A.A) obtained a mixture of metallic copper and cuprous oxide whose characteristic UV–vis absorption peak is around 560 nm, with the average size of Cu₂O NPs ranging between 28 and 12 nm, verified by SEM and TEM analyses. In this synthesis, we describe the

effect of A.A. as a decelerator of the oxidation and agglomeration process. Fourier transform infrared (FTIR) spectra showed the presence of polyhydroxyl structure on the surface of nanoparticulated copper giving an excellent dispersing effect on Cu_2O NPs [17]. However, this traditional chemical synthesis process is being replaced by the green synthesis method. [18,19].

Extracts from six plants, *Eucalyptus camaldulensis, Azadirachta indica, Murraya koenigii, Avicennia marina, Rosa rubiginosa,* and *Datura stramonium*, for example, were used as reducing agents in the Cu_2O NPs synthesis process, showing in their UV–vis characterization plasmon resonance peaks between 563 nm and 582 nm, and confirming by TEM nanoparticle sizes between 29 nm and 48 nm. FTIR characterization reveals that biomolecules such as proteins, polyphenols, and other phytochemical components present in the extracts can act as reducing agents [20]. In the production of copper nanoparticles, the effects of extract concentration, pH and temperature were analyzed, finding that the higher the extract concentration, the longer the wavelength of the copper nanoparticles, the higher the wavelength of the copper nanoparticles of the plasmon resonance peak is shorter in comparison with other concentrations, so it can be stated that particles are smaller in size. Regarding pH and temperature values, smaller nanoparticles are obtained for alkaline pH values (pH 8–10) and temperatures around 60 °C [21].

Current reports show Cu_2O NPs as potential bactericides and fungicides [22–24]. Using eucalyptus (*Eucalyptus globulus* L.) and peppermint (*Mentha piperita*) leaf extracts, Cu_2O NPs were synthesized and characterized obtaining sizes between 10 and 130 nm with eucalyptus extract, and between 23 and 39 nm with peppermint extract; and it was possible to verify their fungicidal action through mycelial inhibition, between 93.75% by CuNP- Eucalyptus leaves 1000 ppm and 99.78% by CuNP-Mint leaves 1000 ppm compared to conventional fungicides 72.82% and 85.85% in carbendazim 500 ppm and copper oxychloride 2500 ppm respectively, against the fungus *Colletotrichum capsici* that affects chili peppers [5]. While Cu_2O NPs sized between 6.93 nm and 20.70 nm obtained with *Citrus sinensis* extract showed a bactericidal capacity against *Escherichia coli* and *Staphylococcus aureus*, as well as a non-cytotoxic nature in the L929 mouse fibroblast cell line by means of the XTT cell viability assay [25].

Complex healthcare contexts have emphasized the development of biocidal materials such as wound dressings based on the impregnation of metallic silver nanoparticles in wool, cotton, viscose, nylon, and polyamide [26–28]. In a bandage evaluation by impregnation of cotton fabric with crystalline silver nanoparticles and bimetallic Ag/Cu composites, the antimicrobial properties of silver and antifungal properties of bimetallic fabrics were confirmed for a wide range of multi-resistant bacteria and fungi such as *Enterobacter aerogenes, Proteus mirabilis, Klebsiella pneumoniae, Candida, Albicans* yeasts, and micromycetes [29].

Nanoparticles are also used as composites with essential oils with bactericidal effects, including Gram-positive and Gram-negative bacteria [30].

Microorganism persistence on objects or surfaces is a characteristic of interest when designing products that facilitate the implementation of infection or outbreak control strategies. Recent studies show that factors such as porosity, temperature, light exposure, humidity, and surface type, among others, affect the persistence of pathogens in the environment [31]. Thus, the survival of SARS-CoV was compared between two different hospital safety gowns: a disposable, fluid-repellent gown and a cotton gown. It was determined that the cotton material immediately absorbed the droplets containing a high concentration of virus culture, and one hour later no active virus was detected, whereas most of the virus remained viable on disposable gowns for up to 24 h. Therefore, a fluid-absorbent outer layer on PPE (Personal protection equipment) - designed garments and medical devices may be advantageous [32]. A more recent study shows that, at 21–23 °C and a relative humidity of 40%, both SARS-CoV-1 and SARS-CoV-2 coronaviruses appeared to be more persistent on cardboard compared to non-absorbent materials such as plastic and stainless steel [33].

This research makes a comparative evaluation of the potential of copper nanoparticles (Cu_2O NPs) synthesis processes through the chemical route (using ascorbic acid as reductant) and the green route (using for the first time the extract of *Myrciaria dubia* fruit as reductant), considering in both cases the influence of the reductant volume. Likewise, based on the best result in each case, it has been applied in the functionalization of textiles (Cu_2O NPs impregnation) following two methods (in situ and post-synthesis), which have been subsequently evaluated for their antimicrobial and antifungal capacity. This application appears as a potential alternative for applications in the health sector, offering an evaluation of the effectiveness of the organic synthesis process versus a purely synthetic one. This application appears as a potential alternative for applications in the health sector, offering an evaluation of the effectiveness of the organic synthesis process versus a purely synthetic one.

2. Materials and methods

2.1. Materials

Copper sulfate pentahydrate $CuSO_4 5H_2O$ (CAS no. 7758–99–8), sodium hydroxide ACS (CAS no. 1310–73–2), and ascorbic acid (CAS no. 50–81–7) were purchased at Merck Millipore. Ultrapure water (Thermo Scientific, Barnstead Smart2Pure, MA, USA) was used throughout the experiment. *Myrciaria dubia* (camu-camu) fruit was obtained at a local supermarket (Trujillo, Peru) considering only one supplier.

The textile samples used for functionalization had a composition of 70% cotton and 30% polyester with weft and warp-type configuration, with taffeta construction. The textile samples had an area of 120 cm^2 and were carefully washed with distilled water and dried in an oven at 90 °C for 15 min before the Cu_2O NPs impregnation process.

2.2. Synthesis of copper nanoparticles by green and chemical route

2.2.1. Extraction of juice from M. dubia "camu-camu"

The fruits of *M. dubia* were used. To extract the juice, the fruit was washed three times with distilled water. Then, the fruits were crushed using a mortar and pestle, and, finally, the residues -such as the peel- were separated by using vacuum filtration equipment and Whatman No. 1 filter paper. The juice obtained was centrifuged at 5000 rpm for 15 min, at room temperature, to remove heavy biomaterials, and filtered again using Whatman No. 42 filter paper with a vacuum pump. Finally, the juice obtained was stored and left to rest at 4 °C in amber vials, to be used for further experiments.

2.2.2. Synthesis of cuprous oxide nanoparticles (Cu_2O NPs) by the green route

50 mL of 0.05 M copper sulfate pentahydrate solution was prepared and kept at 500 rpm using a magnetic stirrer. Next, 2.5 mL of 7.5 M sodium hydroxide (NaOH) was added dropwise at 1200 rpm. During this phase, the suspension was observed to change from light blue to dark blue. Finally, 3 mL, 5 mL, 8 mL, and 10 mL of *M. dubia* extract were added dropwise at 1200 rpm. The whole process was carried out at room temperature (23 °C). In this last phase, a change from dark blue to different shades ranging from dark orange to light orange was observed, depending on the volume of extract supplied, and indicating the formation of each colloidal solution.

2.2.3. Synthesis of cuprous oxide nanoparticles (Cu_2O NPs) by the chemical route

For the synthesis of copper nanoparticles, the study conducted by Xiong, 2011, was used as a reference [34] with modifications. 450 mL of 0.05 M $CuSO_4 5H_2O$ solution was prepared and stirred at 600 rpm using a magnetic stirrer. Then, 22.5 mL of 7.5 M sodium hydroxide was added dropwise. This mixture was homogenized at 1200 rpm for about 20 min
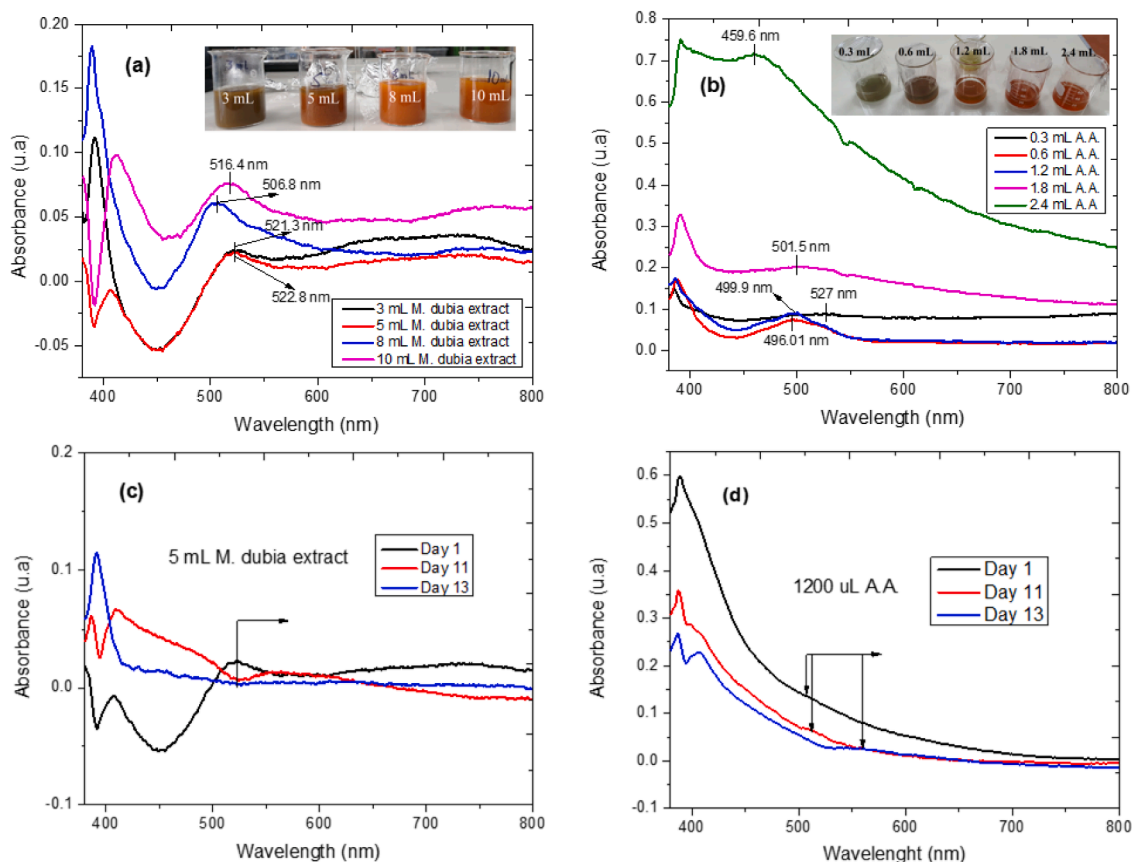
Fig. 1. UV–vis spectra of Cu$_2$O NPs. (a) Influence of the volume of *M. dubia* extract (green synthesis), (b) Influence of A. A. volume (chemical synthesis), (c) Stability over time of Cu$_2$O NPs using 5 mL of *M. dubia* extract, (d) Stability over time of Cu$_2$O NPs using 1200 µL of A.A.

until it became a dark blue mixture, with a viscous consistency. Finally, 300 µL, 600 µL, 1200 µL, 1800 µL, and 2400 µL of 1.13 M ascorbic acid (A.A.) were added and vigorously stirred at 1200 rpm. The whole process was carried out at room temperature (23 °C). In this last phase, a change from dark blue to different shades ranging from dark green to light orange was observed depending on the volume of ascorbic acid supplied, indicating the formation of each colloidal solution.

2.3. Functionalization of textiles

2.3.1. In-situ functionalization of textiles with Cu$_2$O NPs obtained by green and chemical synthesis

The textile functionalization was performed by the exhaustion method and in parallel to the green and chemical Cu$_2$O NPs synthesis process. For this, 900 mL of 0.05 M copper sulfate pentahydrate was prepared and divided into two beakers with volumes of 450 mL each. The solution was stirred (500 rpm) for 10 min. Subsequently, a textile sample was immersed in each beaker and kept stirring for 3 min. Next, 7.5 M (22.5 mL in each beaker) sodium hydroxide was added dropwise (to each sample) with vigorous stirring (1200 rpm), and 90 mL of *M. dubia* juice (for the case of green synthesis), or 27 mL of 1.13 M ascorbic acid (for the case of chemical synthesis). In both cases, it was kept stirring for 10 min. The entire process was carried out at room temperature. Once finished, the textile samples were removed, rinsed with ultrapure water, and left to drain for 10 min. Finally, the samples were placed in an oven at 100 °C for 15 min. The textile samples were placed in sterilized containers.

2.3.2. Post-synthesis functionalization of textiles with Cu$_2$O NPs obtained by green synthesis

Textile functionalization was performed by the exhaustion method,

using the supernatant of Cu$_2$O NPs colloid obtained by the green route, for which the colloid was left to rest for 24 h. 500 mL of colloid contained in a beaker was used; the textile samples were vertically immersed and previously fastened to a support, designed for this purpose. Then, they were stirred at 1200 rpm for 60 min; all this process was done at room temperature. Afterward, the sample was removed and briefly rinsed with ultrapure water to remove any remaining sedimentation. Finally, it was taken to an oven at 100 °C for 15 min. The textile samples were placed in sterilized containers.

2.3.3. Post-synthesis functionalization of textiles with Cu$_2$O NPs obtained by chemical synthesis

Textile functionalization was performed by the exhaustion method, using the supernatant of Cu$_2$O NPs colloid obtained by chemical route, for which the colloid was left to rest for 60 h due to its high density. 450 mL of colloid contained in a beaker was used; the textile samples were vertically immersed and previously fastened to a support, designed for this purpose. Then, a magnetic bar was added to initiate magnetic stirring (900 rpm) for 10 min; all this process was done at room temperature. Afterward, the sample was removed and briefly rinsed with ultrapure water to remove any remaining sedimentation. Finally, it was taken to an oven at 100 °C for 15 min. The textile samples were placed in sterilized containers.
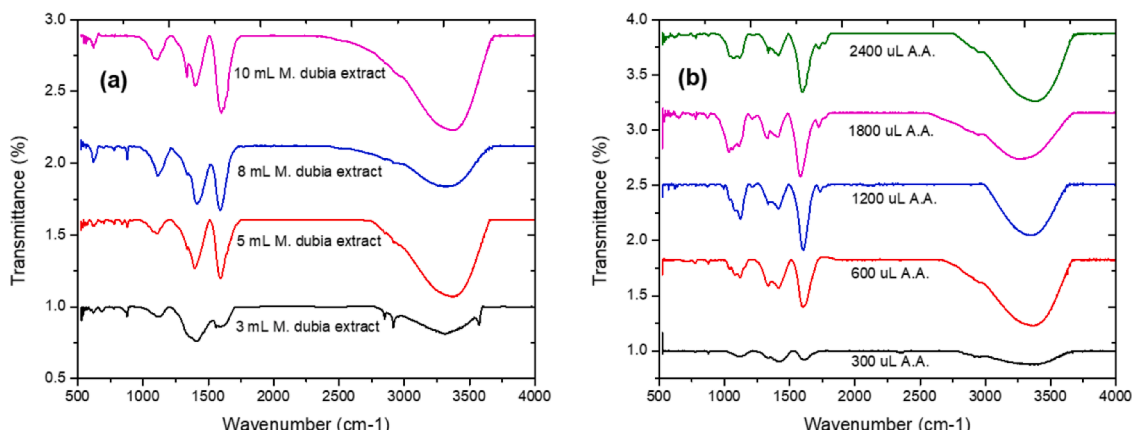
2.4. Characterization of Cu$_2$O NPs and functionalized textiles

2.4.1. Scanning electron microscopy

The textiles were metalized with a thin layer of gold by sputtering, with an exposure time of 180 s at 20 mA. The analyses were performed by a scanning electron microscope of the JSM-6390LV, Jeol, using an acceleration voltage of 20 kV and spot size of 50. EDX measurements

Fig. 2. (a) FTIR spectra of the influence of *M. dubia* extract volume on the green synthesis of Cu₂O NPs, (b) FTIR spectra of the influence of A.A. volume on the chemical synthesis of Cu₂O NPs.

were carried out with the SEM equipped with an OXFORD EDS 7582-M.

2.4.2. Transmission electron microscopy

The particle size and shape of the Cu₂O NPs suspension was done using TEM (JEOL, JEM2011), at an acceleration voltage of 120 kV. Samples were prepared by placing 5 μl of the reaction mixtures on carbon-coated copper grids, followed by drying in a desiccator with silica for 16 h. EDX measurements were carried out with the TEM equipped with an OXFORD EDS 6498.

2.4.3. Dynamic light scattering

The hydrodynamic diameter, zeta potential, and polydispersity of the Cu₂O NPs were determined by dynamic light scattering (DLS), using a Zetasizer Nano Zs90 instrument (Malvern Instruments, UK). The analyses were carried out with a dispersion angle of 90°, at a temperature of 25 °C, using samples diluted (1:3) with Milli-Q water.

2.4.4. Fourier transformed infrared spectroscopy

The main functional groups present in the nanoparticles, the textiles with nanoparticles and the control textiles, were analyzed by FTIR spectroscopic analysis. The samples were analyzed using a Nicolet iS50 FT-IR infrared spectrometer (Thermo Fisher Scientific), in the range of 500–4000 cm^{-1}, with 200 scans per sample.

2.5. Bacterial and fungal test to fabrics with nanoparticles

For the test, 1 mL of bacteria (*E. coli* ATCC No. 8739 and *Staphylococcus aureus* ATCC No. 6538) and fungus (*Aspergillus brasiliensis* ATCC No. 16,404) were used at a concentration of 1×10^5 CFU/mL in buffered solution (9% saline solution) on fabrics functionalized with Cu₂O NPs and negative control fabric with dimensions of 1.75 cm x 2.25 cm side, in sterile 50 mL tubes. Afterward, it was incubated at 35 °C for 24 h. Subsequently, 4 mL of Trypticase Soy Broth medium was added and vortexed at 1200 rpm x 2 min to dislodge the bacteria or fungi impregnated on the fabric, and, then, 1 mL was seeded by the pour plate method for colony counting. Incubation was performed at 35 °C for 24 h for bacteria and yeasts, and at 25 °C for 5 days for filamentous fungi. Each process was performed in triplicate. Finally, counting was performed using a colony counter.

3. Results and discussion

3.1. Synthesis and characterization of Cu₂O NPs

The handling of matter at the nanometric scale allows the evaluation of new characteristics specifically related to the size and, in turn, related to optical properties, in which there are also some cases (non-metallic

nanoparticles) showing a exciton resonance [35,36]. In this sense, characterization by UV–vis spectrophotometry appears as a useful technique to evaluate the position and shape of the exciton transition peaks of nanoparticulated colloids.

The formation of nanoparticles was initially verified by the color change after adding the reducing agent. This is in response to the exciton transition peak and the ionic reduction process due to the reaction with both the *M. dubia* extract (green method) and ascorbic acid (chemical method). The difference is totally noticeable, which, in turn, is also evident from the influence of the volume of reducing agents. Fig. 1(a) shows the absorbance peaks of the Cu₂O NPs colloid obtained by the green route and its influence on the volume of organic extract, where behaviors such as, the higher the volume, the exciton resonance peak tends more toward the blueshift, and the increase of its absorbance. This is likely related to a decrease in size and higher production of NPs. All exciton resonance peaks are around 506 and 522 nm.

Fig. 1(b) shows the absorbances of the Cu₂O NPs colloid obtained by chemical route, specifically the influence of the volume of reductant A. A. The weak presence of the exciton transition peak is evident, and, in some cases, with higher bandwidth, which would indicate that they are highly polydisperse Cu₂O NPs. Likewise, the general range of peak is between 459 and 527 nm.

In both syntheses, peaks around 380 nm can be evidenced. This value is linked to the oxidation of ascorbic acid present in the extract (and motivated by the presence of water in the extract) and chemical ascorbic acid (due to the water contained in the solvent), forming H₂O₂ molecules [34]. For the functionalization of textiles, only colloids synthesized using 5 mL of *M. dubia* extract and 1200 μL of A.A. were considered. The former, due to having an exciton resonance peak within the established range for this type of nanomaterial, also, for having a high monodispersity (information that will be reinforced with TEM analysis); the latter, obtained by chemical method, was considered because it showed a better presence of exciton transition peak and with better size dispersion.

Figs. 1(c) and (d) show the evaluation of stability over time from 1 to 13 days for the colloids synthesized using 5 mL of *M. dubia* extract and 1200 μL of A.A. A minimal shift of the exciton transition can be observed for the first case, which would indicate better stability between the two syntheses. For the second case, there is a greater dynamic where the longer the time there is a shift of the exciton transition toward the redshift, which would indicate an increase and/or formation of aggregates or clusters; this reinforced with the decrease of the absorbance, which would indicate, in general terms, that the chemical synthesis had a more complete reaction, but obtaining Cu₂O NPs with sufficient surface charge to generate agglomerates. It should be noted that the textiles were treated with the aforementioned colloids on the same day of the synthesis.
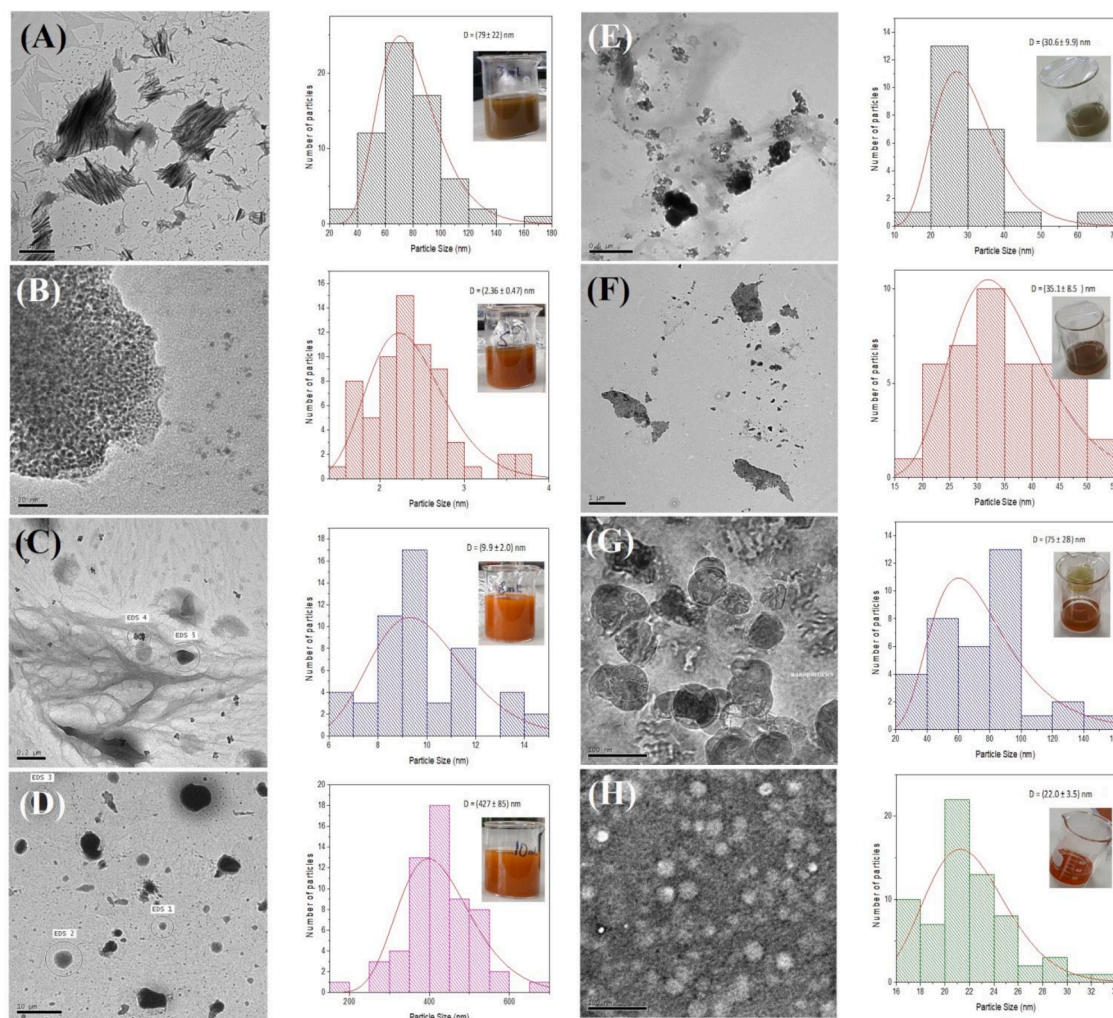
Fig. 3. TEM images and distribution of Cu$_2$O NPs particle size, and the influence of volume variation of the green reductant (*M. dubia*): (A) 3 mL, (B) 5 mL, (C) 8 mL, and (D) 10 mL; and the chemical reductant (Ascorbic Acid): (E) 300 μL, (F) 600 μL, (G) 1200 μL, and (H) 2400 μL.

To identify functional groups of the molecules responsible for the synthesis and stabilization of Cu$_2$O NPs, a FTIR spectroscopic analysis was performed on biosynthesized (Fig. 2a) and chemically synthesized Cu$_2$O NPs (Fig. 2b). In the biosynthesized Cu$_2$O NPs, the FTIR measurements (Fig. 2a) help to identify possible biomolecules present in the plant extract that act as reducing and capping agents. The absorption at 3000–3350 cm^{-1} has been ascribed to stretching O—H vibrations [37–41]. It can be observed that this peak is more prominent after the 5 mL of *M. dubia* extract. The peaks at 1580–1620 cm^{-1} and 1378–1416 cm^{-1} correspond to the asymmetric and symmetric vibration of carboxylates (COO$^-$), respectively [42,43]. Absorption peaks in the range of 877–879 cm^{-1}, present in the Cu$_2$O NPs synthesized with 3–8 mL of *M. dubia* extract, have been attributed to aromatic C—H bending [37,42]. The band at 620 cm^{-1} is assigned to Cu(I)–O vibration of Cu$_2$O NPs [44–46]. The peaks corresponding to C=C, C=O, and C–H have been reported to come from phytochemicals such as flavonoids that are contained in plant juice.

Otherwise, Cu$_2$O NPs (Fig. 2b), synthesized by chemical route, show absorption peaks in the range of 3267–3370 cm^{-1} which corresponds to OH stretching, present as a result of the hydroxyl group on the surface of Cu$_2$O [47]. The peaks at 1558–1615 cm^{-1} and 1395–1417 cm^{-1} correspond to carboxylate vibrations (COO$^-$), as previously described in Fig. 2a [42]. Absorption peaks in the range of 1035–1119 cm^{-1} are attributed to C—O stretching of primary and secondary alcohol [48]. The band at 617–651 cm^{-1} is assigned to Cu–O stretching vibration

[49].

Transmission electron microscopy (TEM) was used to evaluate the size, distribution, and morphology of nanoparticles obtained by both methods. Fig. 3 shows the results. In general, significant differences can be seen both in the influence of the volume of the organic (extract) and inorganic (ascorbic acid) reductant, as well as between each group, considering the best syntheses: 5 mL extract and 1200 μL A.A.

In the green synthesis group, the relationship between the results from spectrophotometry, FTIR, and TEM images is evident. Fig. 3A, C, and D show little nanostructure formation and high trace content (densities) coming from the extract, which is in relationship with the vibrations of aromatic C—H groups found by FTIR; the sizes of the nanostructures are 79 ± 22 nm, 9.9 ± 2.0 nm, and 427 ± 85 nm, respectively. An important detail to highlight is the high polydispersity present in the aforementioned samples. On the contrary, Fig. 3b (using 5 mL extract) shows nanoparticles of 2.36 ± 0.47 nm, with defined spherical geometry, high monodispersity, and absence of organic traces, which is confirmed by the vibrations found through FTIR, and the exciton resonance peaks of the spectrophotometric results. This has implications for the size stability over time, where there is a good relationship between proportional contributions of hydroxide ions (OH) from the extract and their interaction with the metal ions of the precursor, precisely. Fig. 2a shows that, for 5 mL extract, the peak within the range 3000–3350 cm^{-1} is more intense, and this is related to the presence of the OH functional group, which has generated a correct
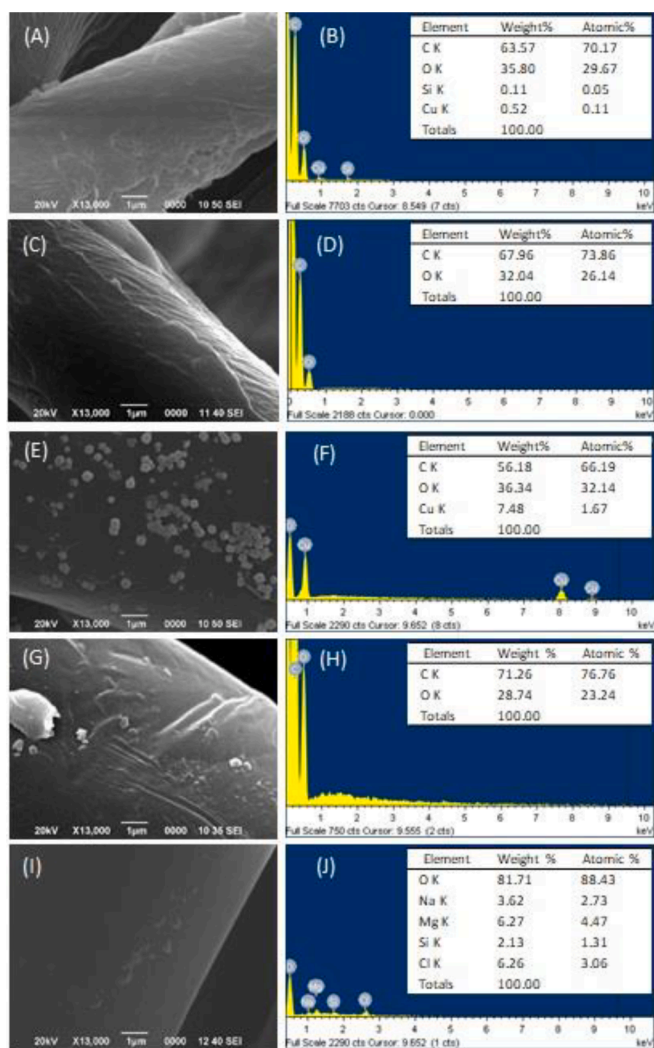
Fig. 4. Characterization by SEM (A,C,E,G and I) and EDX spectrometry (B,D,F, H and J) of textiles functionalized with Cu$_2$O NPs, obtaining the best characteristics by green method and impregnation treatment: (A,B) In situ, (C,D) Post-synthesis; and chemical method: (E,F) In Situ, (G,H) Post-synthesis. (I,J) Control textile.

chelating effect, favoring the formation of the copper-phenolate complex.

Regarding the group of nanostructures obtained by chemical synthesis, those that comply with parameters such as stability over time, defined geometry, and low trace content have been considered an

efficient process for the formation of nanoparticles. Thus, Fig. 3E, F, and H show the protocols using 300 μL, 600 μL, and 2400 μL, achieving average sizes of 30.6 ± 9.9 nm, 35.1 ± 8.5, and 22.0 ± 3.5 nm, respectively. The aforementioned samples in the 300 and 600 μL volumes have shown a low relationship of Cu$_2$O NPs production. Fig. 3G shows the colloid obtained by using 1200 μL A.A. where nanoparticles with an average size of 75 ± 28 nm have been obtained. Although there is indeed polydispersity, this is the sample that has better stability (Fig. 1d), better defined spherical geometry, and less presence of other functional groups (Fig. 2b).

Both synthesis protocols shown in this research are presented as alternatives that successfully achieve the production of Cu$_2$O NPs. However, it is important to establish the influence criterion of the reductant volume in order to find the optimal reduction relationship and, at the same time, with the least number of final traces in the colloid, which can later hinder the applications.

As for the formation mechanism of the nanostructure, it is produced by a complexation process where the precursor interacts with its Cu^{2+} ion and the juice of *M. dubia*, the latter contains charged biomolecules which act by neutralizing the positive charges of the copper(II) ion, generating a redox process by electron transfer from organic molecules (that are oxidized) to the Cu^{2+} ions that are reduced. The FTIR results show evidence of the presence of hydroxyl group (-OH) and carbonyl group (C=O), which is possibly associated with the presence of the amino acid as a biomolecule containing carboxyl group (-COOH), and the presence of carboxylic acid. Likewise, the phenolic group is also present, as an aromatic organic compound which also contains hydroxyl group, which contributes to the mechanism of nanostructure formation. Thus, ascorbic acid (A.A.) plays a fundamental role, where it forms a conjugated system based on the pairs of hydroxyl group and carbonyl bonds. When synthesizing nanoparticles with the chemical method, A.A. is used directly; however, in the green route method, the juice of the fruit of *M. dubia*, which has a high content of this type of organic acid, has been used.

At the level of the formation process, it is important to highlight that the Cu^{2+} ions have formed cuprous oxide (Cu$_2$O) or copper(I) oxide, a clear example of this is the typical orange color which can be observed in Fig. 1.

3.2. Antimicrobial and antifungal activity from the functionalization of textiles with Cu$_2$O NPs

Copper is widely known to be a biocidal material, as copper ions (Cu^{+2}) have been used for decades to disinfect solids, liquids, and even human tissues. Today, it is used to purify water and as a fungicide [50]. Copper has also been evaluated on metal surfaces developed with this material at a macroscopic size and has been shown to have excellent properties to reduce bacterial viability [51,52]. In that sense, this research applies Cu$_2$O NPs in the functionalization of textiles using the
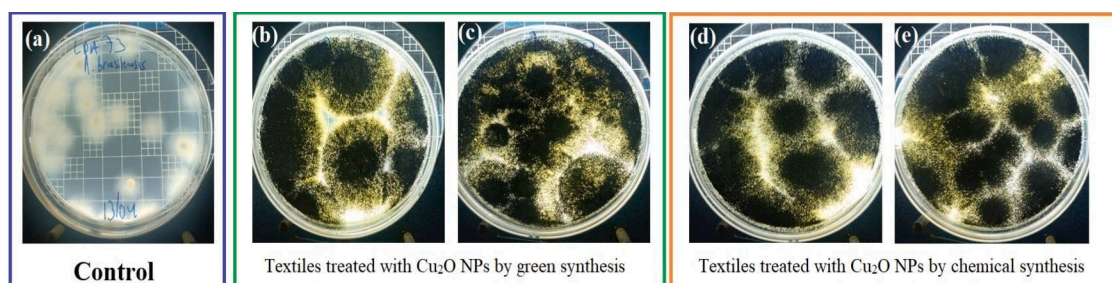
Fig. 5. Evaluation by growth of colony forming units (CFU) of the antifungal activity of textiles functionalized with Cu$_2$O NPs depending on the type of synthesis and the type of textile impregnation. Biological culture control sample (a) *A. brasiliensis*. Group of textiles treated with Cu$_2$O NPs obtained by green route with variation in the impregnation methodology (b) *A. brasiliensis* in textile treated in situ, (c) *A. brasiliensis* in textile treated post-synthesis. Group of textiles treated with Cu$_2$O NPs obtained by chemical route, according to the type of impregnation (d) *A. brasiliensis* in textile treated In Situ (e) *A. brasiliensis* in textile treated post-synthesis. The quantitative values shown in the figure regarding the CFU (Colony Forming Units) were used in the analysis of variance shown in Table 2.
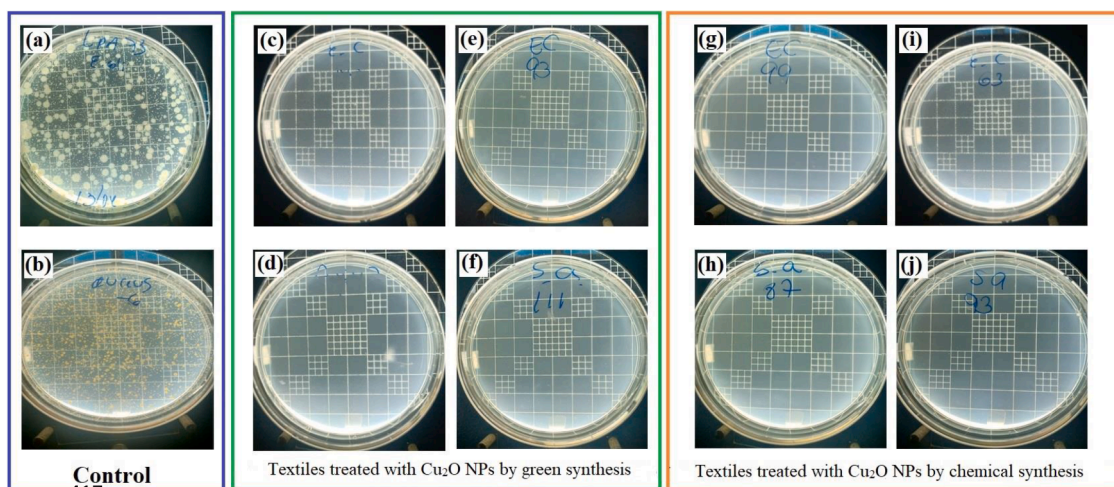
Fig. 6. Evaluation by growth of colony forming unit (CFU) of the antibacterial activity of textiles functionalized with Cu$_2$O NPs according to the type of synthesis and the type of textile impregnation. Biological culture control samples (a) *E. coli*, (b) *S. aureus*. Group of textiles treated with Cu$_2$O NPs obtained by green route, but with variation in the impregnation methodology (c) *E. coli* in textile treated in situ, (d) *S. aureus* in textile treated in situ, (e) *E. coli* in textile treated post-synthesis, (f) *S. aureus* in textile treated post-synthesis Group of textiles treated with Cu$_2$O NPs obtained by chemical route, according to the type of impregnation (g) *E. coli* in textile treated in Situ, (h) *S. aureus* in textile treated in Situ, (i) *E. coli* in textile treated post-synthesis, (j) *S. aureus* in textile treated post-synthesis. The quantitative values shown in the figure regarding the CFU (Colony Forming Units) were used in the analysis of variance shown in Table 1.

nanostructured material with better characteristics obtained and evaluated in the previous section, i. e., with the green method, using 5 mL of *M. dubia* extract as reductant; and, with the chemical method, using 1200 µL of A.A. From this, the influence of the type of textile impregnation was also evaluated, i.e., 'in situ' for the methodology where the textile was submerged from the beginning of the mixture of precursor and reductant, forming Cu$_2$O NPs with the textile submerged; and 'post-synthesis' where the impregnation followed the synthesis of nanoparticles. In all cases, textile samples at a concentration of 70% cotton and 30% polyester were used.

The functionalized textiles were initially characterized by the EDS technique. Fig. 4 shows the results obtained, where the presence of copper can be evidenced in the textiles treated 'in situ' (Fig. 4B and F) regardless of the synthesis method applied to obtain the Cu$_2$O NPs. In the Cu$_2$O NPs synthesized with the green method, a small amount (0.11%), the element Si was detected which could be related to the presence of this element in the extract of *M. dubia*. The case is different for the 'post-synthesis' functionalization protocol (Fig. 4D and H) where there is no presence of Cu$_2$O NPs. This is an indicator that the adhesion of nanostructured material on textile fibers occurs more efficiently during the formation of nanostructures. Fig. 4I shows the control textile, wich does not show the presence of Cu, however, other elements such as Mg, Si, Na, and Cl, were detected in small amount due to interactions during textile processing in bleaching processes and the use of polyester by 30%.

The success of the synthesis process has been demonstrated by the antimicrobial activity (Gram-positive and Gram-negative bacteria, and fungi) of textiles impregnated with Cu$_2$O NPs. In this case, the results obtained are presented (Figs. 5 and 6).

It was observed that all the fabrics functionalized with Cu$_2$O NPs had a 100% inhibition of bacterial growth with a significant difference (*=*p* < 0.05) compared to the fabric control (without nanoparticles). Both the reductant with the green method with nanoparticles of spherical-defined geometry averaging 2.36 ± 0.47 nm (*M. dubia* in In-situ and Post synthesis) and that with the chemical method of ascorbic acid with no defined geometry averaging 75 ± 28 nm, had 100% inhibition. Likewise, there was no difference in the in situ or post-synthesis impregnation of nanoparticles, and, in both cases, there was also 100% inhibition.

As observed for *A. brasiliensis* there was a significant difference ("a, b, c, d" = *p* < 0.05) between all the fabrics treated with nanoparticles and the control fabric without nanoparticles. Besides, it was observed that

Table 1
Effect of cuprous oxide nanoparticles (734 ppm) against *E. coli* and *S. aureus*.

	Fabric control (CFU/mL)	(*M. dubia*/In situ)	(*M. dubia*/Post synthesis)	(Ascorbic acid/ In situ)	(Ascorbic acid/Post synthesis)
E. coli ATCC 8739	*1864 ± 396	*0 (100%)	*0 (100%)	*0 (100%)	*0 (100%)
S. aureus ATCC 6538	*269 ± 97	*0 (100%)	*0 (100%)	*0(100%)	*0 (100%)

there was a significant difference, regarding the moment of the impregnation of nanoparticles, between the in-situ treatment and the post-synthesis treatment, having the highest percentage of inhibition that one of in situ treated fabrics.

A previous study used a combination of copper nanoparticles and essential oils with an inhibitory effect on the growth of *S. aureus* and *E. coli.* [30]. Another study showed that 2.3×10^7 CFU/mL *E. coli* cells were destroyed after 2 h of exposure to cuprous oxide nanoparticles at a concentration of 1 mg/mL while 1.4×10^7 CFU/mL *E. coli* cells were killed after 30 min of exposure to 0.5 mg/mL of Cu(I) and/or Cu(II) oxides. The reaction mechanism of cuprous oxide was lipoperoxidation, generation of reactive oxygen species, protein oxidation, and degradation of bacterial cell DNA [53,54].

In the case of *S. aureus*, a previous study on copper(II) oxide nanoparticles demonstrated the penetration of nanoparticles altering the reductase activity of the bacteria and destroying the bacterial cell membrane [55]. Previous studies have already demonstrated the good activity of cuprous oxide against *E. coli* and *S. aureus* [56]. In our study, all fabrics with nanoparticles, whether treated with the reductant *Myrciaria dubia* "camu-camu" or ascorbic acid, and whether in situ or post-synthesis impregnation of nanoparticles, showed a 100% inhibition of bacterial growth, being significant when compared to the control fabric without nanoparticles (Table 1), showing the powerful antibacterial effect of copper supported by previous studies, and being important to note that *E. coli* and *S. aureus* are among the Gram-negative and Gram-positive bacteria that stand out for being highly involved in nosocomial and dermal infections of great importance to public health, so the 100% antibacterial effect in our study is relevant to fight this type

Table 2

Effect of cuprous oxide nanoparticles (734 ppm) against *A. brasiliensis*.

	Fabric control (CFU/ mL)	(*M. dubia* / In Situ)	(*M. dubia* / Post synthesis)	(Ascorbic acid/ In situ)	(Ascorbic acid/Post synthesis)
A. brasiliensis* ATCC *16,404	("a") 21 ± 4	("a, b, e") 10 ± 1 (52.38%)	("a, b, c") 14 ± 1 (33.33%)	("a, c, d") 10.6 ± 0.6 (49.52%)	("a, d, e") 14.6 ± 0.6 (30.48%)

of bacteria, whether in creams or other products [53–56].

Previous studies have shown the antifungal effect of lipid nanoparticles against Candida with remarkable antifungal effects even in biofilms [57–59]. However, in the case of the antifungal effect of cuprous oxide nanoparticles against a filamentous fungus such as *A. brasiliensis*, our study is pioneering and promising, showing a significant antifungal effect of all fabrics with nanoparticles of between 30.48% and 52.38% inhibition (Table 2), either using the reductant *Myrciaria dubia* "camu-camu" or ascorbic acid, and either in Situ or post-synthesis impregnation of nanoparticles, when compared to the control fabric without nanoparticles. In contrast, there was a significant difference between In Situ treatment and Post Synthesis treatment, the former being the best one with antifungal effect. Therefore, our study certifies the promising use of cuprous oxide to combat infections caused by aspergillosis, which have a high level of morbimortality [60].

4. Conclusions

A novel synthesis of cuprous oxide nanoparticles (Cu$_2$O NPs) was developed by a green route, highlighting the role of *M. dubia* extract as an organic reductant, which, in turn, has managed to overcome the characteristics of the nanomaterial in comparison to those obtained by chemical route. The results obtained by FTIR spectroscopy show the mechanism of nanomaterial formation, being the phenol group the one in charge of reducing the precursor. Likewise, the presence of the OH group is verified, which has generated a correct chelating effect, favoring the formation of the copper-phenolate complex. The best synthesis of Cu$_2$O NPs by green route has resulted using 5 mL of *M. dubia* juice, achieving nanoparticles with spherical morphology and 2.4 ± 0.5 nm size. On the contrary, the best method of the chemical route (2400 μL of A.A.) has achieved sizes of 22.0 ± 3.5 nm. Regarding the antibacterial effect (*E. coli* and *S. aureus*) of the fabrics functionalized with Cu$_2$O NPs, all had a 100% inhibitory effect, which was statistically significant compared to the control fabric without nanoparticles. In the case of the antifungal effect (*A. brasiliensis*) all the fabrics with nanoparticles (In Situ/ Post Synthesis - *Myrciaria dubia* "camu-camu"/ascorbic acid) had a significant effect in comparison to the control fabric, although the best antifungal effect was shown in the in-situ method.

Declaration of Competing Interest

The authors declare that they have no known competing financial interests or personal relationships that could have appeared to influence the work reported in this paper.

Data Availability

The data that has been used is confidential.

References

[1] Z. Nakhaeepour, M. Mashreghi, M.M. Matin, A. NakhaeiPour, M.R. Housaindokht, Multifunctional CuO nanoparticles with cytotoxic effects on KYSE30 esophageal cancer cells, antimicrobial and heavy metal sensing activities, Life Sci. 234 (2019), 116758.

[2] L. Barberia-Roque, O.F. Obidi, E. Gámez-Espinosa, M. Viera, N. Bellotti, Hygienic coatings with bioactive nano-additives from *Senna occidentalis*-mediated green synthesis, NanoImpact 16 (2019), 100184.

[3] M. Mohammadpoor, S. Sabbaghi, M.M. Zerafat, Z. Manafi, Investigating heat transfer properties of copper nanofluid in ethylene glycol synthesized through single and two-step routes, Int. J. Refrig. 99 (2019) 243–250.

[4] N.W. Awang, D. Ramasamy, K. Kadirgama, G. Najafi, N.A. Che Sidik, Study on friction and wear of cellulose nanocrystal (CNC) nanoparticle as lubricating additive in engine oil, Int. J. Heat Mass Transf. 131 (2019) 1196–1204.

[5] K.S. Iliger, T.A. Sofi, N.A. Bhat, F.A. Ahanger, J.C. Sekhar, A.Z. Elhendi, A.A. Al-Huqail, F. Khan, Copper nanoparticles: green synthesis and managing fruit rot disease of chilli caused by, Colletotrichum capsici Saudi J. Biol. Sci. 28 (2021) 1477–1486.

[6] Q. Yan, N. Zhi, L. Yang, G. Xu, Q. Feng, Q. Zhang, S. Sun, A highly sensitive uric acid electrochemical biosensor based on a nano-cube cuprous oxide/ferrocene/ uricase modified glassy carbon electrode, Sci. Rep. 10 (2020) 10607.

[7] F. Tahernejad-Javazmi, M. Shabani-Nooshabadi, H. Karimi-Maleh, 3D reduced graphene oxide/FeNi$_3$-ionic liquid nanocomposite modified sensor; an electrical synergic effect for development of tert-butylhydroquinone and folic acid sensor, Compos. Part B Eng. 172 (2019) 666–670.

[8] A. Khodadadi, E. Faghih-Mirzaei, H. Karimi-Maleh, A. Abbaspourrad, S. Agarwal, V.K. Gupta, A new epirubicin biosensor based on amplifying DNA interactions with polypyrrole and nitrogen-doped reduced graphene: experimental and docking theoretical investigations, Sens. Actuators B Chem. 284 (2019) 568–574.

[9] P. Westerhoff, A. Atkinson, J. Fortner, M.S. Wong, J. Zimmerman, J. Gardea-Torresdey, J. Ranville, P. Herckes, Low risk posed by engineered and incidental nanoparticles in drinking water, Nat. Nanotechnol. 13 (2018) 661–669.

[10] J.G. Croissant, K.S. Butler, J.I. Zink, C.J. Brinker, Synthetic amorphous silica nanoparticles: toxicity, biomedical and environmental implications, Nat. Rev. Mater. 5 (2020) 886–909.

[11] D. Reker, Y. Rybakova, A.R. Kirtane, R. Cao, J.W. Yang, N. Navamajiti, A. Gardner, R.M. Zhang, T. Esfandiary, J. L'Heureux, T. von Erlach, E.M. Smekalova, D. Leboeuf, K. Hess, A. Lopes, J. Rogner, J. Collins, S.M. Tamang, K. Ishida, P. Chamberlain, D. Yun, A. Lytton-Jean, C.K. Soule, J.H. Cheah, A.M. Hayward, R. Langer, G. Traverso, Computationally guided high-throughput design of self-assembling drug nanoparticles, Nat. Nanotechnol. 16 (2021) 725–733.

[12] E.A. Mohamed, Green synthesis of copper & copper oxide nanoparticles using the extract of seedless dates, Heliyon 6 (2020) e03123.

[13] V.U. Siddiqui, A. Ansari, R. Chauhan, W.A. Siddiqi, Green synthesis of copper oxide (CuO) nanoparticles by *Punica granatum* peel extract, Mater. Today: Proceedings 36 (2019) 751–755.

[14] R.M. Altuwirqi, A.S. Albakri, H. Al-Jawhari, E.A. Ganash, Green synthesis of copper oxide nanoparticles by pulsed laser ablation in spinach leaves extract, Optik (Stuttg) 219 (2020), 165280.

[15] D. Asmat-Campos, A.C. Abreu, M.S. Romero-Cano, J. Urquiaga-Zavaleta, R. Contreras-Cáceres, D. Delfín-Narciso, L. Juárez-Cortijo, R. Nazario-Naveda, R. Rengifo-Penadillos, I. Fernández, Unraveling the active biomolecules responsible for the sustainable synthesis of nanoscale silver particles through nuclear magnetic resonance metabolomics, ACS Sustain. Chem. Eng. 8 (2020) 17816–17827.

[16] K. Zhao, J. Wang, W. Kong, P. Zhu, Facile Green synthesis and characterization of copper nanoparticles by aconitic acid for catalytic reduction of nitrophenols, J. Environ. Chem. Eng. 8 (2020), 103517.

[17] S. Jain, A. Jain, P. Kachhawah, V. Devra, Synthesis and size control of copper nanoparticles and their catalytic application, Trans. Nonferrous Met. Soc. China 25 (2015) 3995–4000.

[18] Q. Lv, B. Zhang, X. Xing, Y. Zhao, R. Cai, W. Wang, Q. Gu, Biosynthesis of copper nanoparticles using *Shewanella loihica* PV-4 with antibacterial activity: novel approach and mechanisms investigation, J. Hazard. Mater. 347 (2018) 141–149.

[19] M. Nasrollahzadeh, S.S. Momeni, S.M. Sajadi, Green synthesis of copper nanoparticles using *Plantago asiatica* leaf extract and their application for the cyanation of aldehydes using K$_4$Fe(CN)$_6$, J. Colloid Interface Sci. 506 (2017) 471–477.

[20] M.A. Asghar, M.A. Asghar, Green synthesized and characterized copper nanoparticles using various new plants extracts aggravate microbial cell membrane damage after interaction with lipopolysaccharide, Int. J. Biol. Macromol. 160 (2020) 1168–1176.

[21] S. Amaliyah, D.P. Pangesti, M. Masruri, A. Sabarudin, S.B. Sumitro, Green synthesis and characterization of copper nanoparticles using *Piper retrofractum Vahl* extract as bioreductor and capping agent, Heliyon 6 (2020) e04636.

[22] G. Wang, K. Zhao, C. Gao, J. Wang, Y. Mei, X. Zheng, P. Zhu, Green synthesis of copper nanoparticles using green coffee bean and their applications for efficient reduction of organic dyes, J. Environ. Chem. Eng. 9 (2021), 105331.

[23] S.C. Mali, A. Dhaka, C.K. Githala, R. Trivedi, Green synthesis of copper nanoparticles using *Celastrus paniculatus* Willd. leaf extract and their photocatalytic and antifungal properties, Biotechnol. Reports 27 (2020) e00518.

[24] E. Benassai, M. Del Bubba, C. Ancillotti, I. Colzi, C. Gonnelli, N. Calisi, M. C. Salvatici, E. Casalone, S. Ristori, Green and cost-effective synthesis of copper nanoparticles by extracts of non-edible and waste plant materials from *Vaccinium* species: characterization and antimicrobial activity, Mater. Sci. Eng. C 119 (2021), 111453.

[25] I. Jahan, F. Erci, I. Isildak, Facile microwave-mediated green synthesis of non-toxic copper nanoparticles using *Citrus sinensis* aqueous fruit extract and their antibacterial potentials, J. Drug Deliv. Sci. Technol. 61 (2021), 102172.

[26] S. Mura, G. Greppi, L. Malfatti, B. Lasio, V. Sanna, M.E. Mura, S. Marceddu, A. Lugliè, Multifunctionalization of wool fabrics through nanoparticles: a chemical route towards smart textiles, J. Colloid Interface Sci. 456 (2015) 85–92.

[27] C. Bianco, S. Kezic, M. Crosera, V. Svetličić, S. Šegota, G. Maina, C. Romano, F. Larese, G. Adami, In vitro percutaneous penetration and characterization of silver from silver-containing textiles, Int. J. Nanomedicine 10 (2015) 1899–1908.

[28] M. Jabli, Y.O. Al-Ghamdi, N. Sebeia, S.G. Almalki, W. Alturaiki, J.M. Khaled, A. S. Mubarak, F.K. Algethami, Green synthesis of colloid metal oxide nanoparticles using *Cynomorium coccineum*: application for printing cotton and evaluation of the antimicrobial activities, Mater. Chem. Phys. 249 (2020), 123171.

[29] A.M. Eremenko, I.S. Petrik, N.P. Smirnova, A.V Rudenko, Y.S. Marikvas, Antibacterial and antimycotic activity of cotton fabrics, impregnated with silver and binary silver/copper nanoparticles, Nanoscale Res. Lett. 11 (2016) 28.

[30] Y. Jiang, D. Wang, F. Li, D. Li, Q. Huang, Cinnamon essential oil Pickering emulsion stabilized by zein-pectin composite nanoparticles: characterization, antimicrobial effect and advantages in storage application, Int. J. Biol. Macromol. 148 (2020) 1280–1289.

[31] P.D. Rakowska, M. Tiddia, N. Faruqui, C. Bankier, Y. Pei, A.J. Pollard, J. Zhang, I. S. Gilmore, Antiviral surfaces and coatings and their mechanisms of action, Commun. Mater. 2 (2021) 53.

[32] M.Y.Y. Lai, P.K.C. Cheng, W.W.L. Lim, Survival of severe acute respiratory syndrome coronavirus, Clin. Infect. Dis. 41 (2005) 67–71.

[33] N. Van Doremalen, T. Bushmaker, D.H. Morris, M.G. Holbrook, A. Gamble, B. N. Williamson, Azaibi Tamin, Jennifer L. Harcourt, N.J. Thornburg, S.I. Gerber, J. O. Lloyd-Smith, E. Wit, V.J Munster, Aerosol and surface stability of SARS-CoV-2 as compared with SARS-CoV-1, N. Engl. J. Med. 382 (2020) 1564–1567.

[34] J. Xiong, Y. Wang, Q. Xue, X. Wu, Synthesis of highly stable dispersions of nanosized copper particles using L-ascorbic acid, Green Chem. 13 (2011) 900–904.

[35] S.K. Islam, M.A. Sohel, J.R. Lombardi, Coupled exciton and charge-transfer resonances in the Raman enhancement of phonon modes of CdSe quantum dots (QDs), J. Phys. Chem. C 118 (2014) 19415–19421.

[36] A.A. Kamnev, P.V. Mamchenkova, Y.A. Dyatlova, A.V Tugarova, FTIR spectroscopic studies of selenite reduction by cells of the rhizobacterium *Azospirillum brasilense* Sp7 and the formation of selenium nanoparticles, J. Mol. Struct. 1140 (2017) 106–112.

[37] M. Rafique, F. Shafiq, S.S. Ali Gillani, M. Shakil, M.B. Tahir, I. Sadaf, Eco-friendly green and biosynthesis of copper oxide nanoparticles using *Citrofortunella microcarpa* leaves extract for efficient photocatalytic degradation of Rhodamin B dye form textile wastewater, Optik (Stuttg) 208 (2020), 164053.

[38] P. Vanathi, P. Rajiv, R. Sivaraj, Synthesis and characterization of *Eichhornia*-mediated copper oxide nanoparticles and assessing their antifungal activity against plant pathogens, Bull. Mater. Sci. 39 (2016) 1165–1170.

[39] P. Yugandhar, T. Vasavi, P. Uma Maheswari Devi, N. Savithramma, Bioinspired green synthesis of copper oxide nanoparticles from *Syzygium alternifolium* (Wt.) Walp: characterization and evaluation of its synergistic antimicrobial and anticancer activity, Appl. Nanosci. 7 (2017) 417–427.

[40] A. Bashiri Rezaie, M. Montazer, M. Mahmoudi Rad, Biosynthesis of nano cupric oxide on cotton using *Seidlitzia rosmarinus* ashes utilizing bio, photo, acid sensing and leaching properties, Carbohydr. Polym. 177 (2017) 1–12.

[41] M. Hosseini-Koupaei, B. Shareghi, A.A. Saboury, F. Davar, V.A. Sirotkin, M. H. Hosseini-Koupaei, Z. Enteshari, Catalytic activity, structure and stability of proteinase K in the presence of biosynthesized CuO nanoparticles, Int. J. Biol. Macromol. 122 (2019) 732–744.

[42] A.A. Kamnev, Y.A. Dyatlova, O.A. Kenzhegulov, A.A. Vladimirova, P. V. Mamchenkova, A.V. Tugarova, Fourier transform infrared (FTIR) spectroscopic analyses of microbiological samples and biogenic selenium nanoparticles of microbial origin: sample preparation effects, Molecules 26 (2021) 1146.

[43] J. Sackey, A.C. Nwanya, A.K.H. Bashir, N. Matinise, J.B. Ngilirabanga, A.E. Ameh, E. Coetsee, M. Maaza, Electrochemical properties of *Euphorbia pulcherrima* mediated copper oxide nanoparticles, Mater. Chem. Phys. 244 (2020), 122714.

[44] K. Gopalakrishnan, C. Ramesh, V. Ragunathan, M. Thamilselvan, Antibacterial activity of Cu$_2$O nanoparticles on *E. coli* synthesized from *Tridax procumbens* leaf extract and surface coating with polyaniline, Dig. J. Nanomater. Biostructures 7 (2012) 833–839.

[45] F. Erci, R. Cakir-Koc, M. Yontem, E. Torlak, Synthesis of biologically active copper oxide nanoparticles as promising novel antibacterial-antibiofilm agents, Prep. Biochem. Biotechnol. 50 (2020) 538–548.

[46] D. Renuga, J. Jeyasundari, Y. Shakthi Athithan A S y Brightson Arul Jacob, Synthesis and characterization of copper oxide nanoparticles using *Brassica oleracea var. italic* extract for its antifungal application, Mater. Res. Express 7 (2020), 045007.

[47] H. Siddiqui, M.S. Qureshi, F.Z. Haque, Surfactant assisted wet chemical synthesis of copper oxide (CuO) nanostructures and their spectroscopic analysis, Optik (Stuttg) 127 (2016) 2740–2747.

[48] A.A. Badawy, N.A.H. Abdelfattah, S.S. Salem, M.F. Awad, A. Fouda, Efficacy assessment of biosynthesized copper oxide nanoparticles (CuO-NPs) on stored grain insects and their impacts on morphological and physiological traits of wheat (*Triticum aestivum* L.), Plant *Biol.* 10 (2021) 233.

[49] S. Sagadevan, S. Vennila, A.R. Marlinda, Y. Al-Douri, M.R. Johan, J. Anita Lett, Synthesis and evaluation of the structural, optical, and antibacterial properties of copper oxide nanoparticles, Appl. Phys. A 125 (2019) 489.

[50] G. Borkow, J. Gabbay, Copper as a biocidal tool, Curr. Med. Chem. 12 (2005) 2163–2175.

[51] S.A. Wilks, H. Michels, C.W. Keevil, The survival of *Escherichia coli* O157 on a range of metal surfaces, Int. J. Food Microbiol. 105 (2005) 445–454.

[52] J.O. Noyce, H. Michels, C.W. Keevil, Potential use of copper surfaces to reduce survival of epidemic meticillin-resistant *Staphylococcus aureus* in the healthcare environment, J. Hosp. Infect. 63 (2006) 289–297.

[53] P. Pandey, M.S. Packiyaraj, H. Nigam, G.S. Agarwal, B. Singh, M.K. Patra, Antimicrobial properties of CuO nanorods and multi-armed nanoparticles against *B. anthracis* vegetative cells and endospores, Beilstein J. Nanotechnol. 5 (2014) 789–800.

[54] A.K. Chatterjee, R. Chakraborty, T. Basu, Mechanism of antibacterial activity of copper nanoparticles, Nanotechnology 25 (2014), 135101.

[55] Y.H. Hsueh, P.H. Tsai, K.S. Lin, pH-dependent antimicrobial properties of copper oxide nanoparticles in *Staphylococcus aureus*, Int. J. Mol. Sci. 18 (2017) 793.

[56] A. Azam, A.S. Ahmed, M. Oves, M.S. Khan, A. Memic, Size-dependent antimicrobial properties of CuO nanoparticles against Gram-positive and -negative bacterial strains, Int. J. Nanomedicine 7 (2012) 3527–3535.

[57] B.S. Fazly Bazzaz, B. Khameneh, N. Namazi, M. Iranshahi, D. Davoodi, S. Golmohammadzadeh, Solid lipid nanoparticles carrying *Eugenia caryophyllata* essential oil: the novel nanoparticulate systems with broad-spectrum antimicrobial activity, Lett. Appl. Microbiol. 66 (2018) 506–513.

[58] M.E. de Souza, D.J. Clerici, C.M. Verdi, G. Fleck, P.M. Quatrin, L.E. Spat, P. C. Bonez, C F dos Santos, R.P. Antoniazzi, F.B. Zanatta, A. Gundel, D.S.T. Martinez, R. de Almeida Vaucher, R.C.V. Santos, Antimicrobial activity of *Melaleuca alternifolia* nanoparticles in polymicrobial biofilm in situ, Microb. Pathog. 113 (2017) 432–437.

[59] P. Piran, H.S. Kafil, S. Ghanbarzadeh, R. Safdari, H. Hamishehkar, Formulation of menthol-loaded nanostructured lipid carriers to enhance its antimicrobial activity for food preservation, Adv. Pharm. Bull. 7 (2017) 261–268.

[60] G.E. Hayes, L. Novak-Frazer, Chronic pulmonary aspergillosis-where are we? And where are we going? J. Fungi (Basel, Switzerland) 2 (2016) 18.